

# Zoonotic Threat of G4 Genotype Eurasian Avian-Like Swine Influenza A(H1N1) Viruses, China, 2020

Min Gu,<sup>1</sup> Kaibiao Chen,<sup>1</sup> Zhichuang Ge, Jun Jiao, Tianyu Cai, Suhan Liu, Xiaoquan Wang, Xinan Jiao, Daxin Peng, Xiufan Liu

We investigated genetic and biologic characteristics of 2 Eurasian avian-like H1N1 swine influenza viruses from pigs in China that belong to the predominant G4 genotype. One swine isolate exhibited strikingly great homology to contemporaneous human Eurasian avian-like H1N1 isolates, preferential binding to the human-type receptor, and vigorous replication in mice without adaptation.

Pigs have long been considered a crucial genetic mixing vessel for influenza A viruses (IAVs) of different hosts (1) because of the dual expression of human (SA $\alpha$ -2,6Gal) and avian (SA $\alpha$ -2,3Gal) viral receptors on their respiratory epithelium. Swine IAVs such as H1N1 and H3N2 subtypes sporadically infect humans and are prone to cause bidirectional interspecies transmission at the swine-human interface (2-5). So far, Eurasian avian-like (EA) H1N1 has dominated prevalence in pig herds in China and caused >10 human infections (6-9). In particular, the dominant genotype 4 (G4) EA H1N1 containing 2009 pandemic influenza A(H1N1) polymerase basic (PB) 1 and 2, polymerase acid (PA), nucleoprotein (NP), and matrix (M) genes, plus the triple-reassortant (TR) nonstructural (NS) gene, is thought to be a candidate virus of potential pandemic (10,11). Indeed, a case of human infection with G4 EA H1N1 was reported in Yunan Province, China, in 2021 (8). It is imperative to conduct surveillance on swine IAVs and evaluate their risk to public health.

## The Study

During monthly surveillance of swine IAVs in China during October-December 2020, we collected a total

of 376 nasal swab samples from apparently healthy pigs in a slaughterhouse accommodating swine from neighboring regions (Jiangsu, Shandong, and Anhui Provinces in eastern China). We detected H1 subtype swine influenza virus in 9 of those by real-time reverse transcription quantitative PCR; 2 were confirmed as hemagglutinin (HA) positive after inoculating into MDCK cells (12). We further evaluated these 2 swine IAV isolates, A/swine/Jiangsu/HD11/2020 (H1N1) [HD11] and A/swine/Anhui/HD21/2020 (H1N1) [HD21], for their genetic and biologic characteristics.

The genome sequences of HD11 and HD21 deposited in the GenBank database (accession no. OL744678-93) shared 95.4%-99.0% nucleotide identities across the coding regions of 8 genes. We performed searches of those sequences on BLAST (<https://blast.ncbi.nlm.nih.gov/Blast.cgi>) and the GISAID database (<http://platform.gisaid.org>) to present a more comprehensive scene of the homologous reference influenza viruses. As shown by the closest BLAST hits (Table 1), HD11 and HD21 were not only highly related to swine origin IAVs collected during 2012-2018 but also remarkably similar to contemporaneous human H1N1 isolates from 2020 and 2021.

We constructed a phylogenetic gene tree analysis with H1N1 reference strains to confirm the intimate genetic relationship between these 2 swine IAVs and human viruses (Appendix Figure 1, <https://wwwnc.cdc.gov/EID/article/28/8/21-2530-App1.pdf>). In each tree, HD11 consistently clustered with 3 human H1N1 viruses, A/Tianjin/00030/2020(H1N1), A/Shandong/00204/2021(H1N1), and A/Sichuan/01208/2021(H1N1). As for HD21, the virus aggregated closely with the HD11-involved subbranch in PB2, HA, NP, NA, and M gene trees but gathered more intimately with another 3 human H1N1 viruses containing A/Hubei-Wujiagang/1324/2020(H1N1),

Author affiliations: Yangzhou University, Yangzhou, China (M. Gu, K. Chen, Z. Ge, J. Jiao, T. Cai, S. Liu, X. Wang, X. Jiao, D. Deng, X. Liu); Jiangsu Co-innovation Center for Prevention and Control of Important Animal Infectious Diseases and Zoonoses, Yangzhou (M. Gu, X. Wang, X. Jiao, D. Peng, X. Liu)

DOI: <https://doi.org/10.3201/eid2808.212530>

<sup>1</sup>These authors contributed equally to this article.

**Table 1.** Comparison of 2 G4 Eurasian avian-like H1N1 swine isolates from pigs in China with similar influenza viruses retrieved from the GISAID and GenBank databases\*

Gene and isolate	Most homologous sequence in GISAID				Most homologous sequence in GenBank			
	Virus strain	% Similarity		Virus strain	% Similarity			
		nt	aa		nt	aa		
<b>PB2</b>								
HD11	A/Sichuan/01208/2021(H1N1)	99.25	99.47	A/swine/Liaoning/PJ89/2014(H1N1)	97.72	98.69		
HD21	A/Sichuan/01208/2021(H1N1)	97.11	98.03	A/swine/Liaoning/PJ89/2014(H1N1)	97.54	98.29		
<b>PB1</b>								
HD11	A/Shandong/00204/2021(H1N1)	99.60	100.00	A/swine/Liaoning/CY102/2014(H1N1)	97.98	98.42		
HD21	A/Hubei-Wujiagang/1324/2020(H1N1)	97.58	98.68	A/swine/Liaoning/CY102/2014(H1N1)	97.71	98.68		
<b>PA</b>								
HD11	A/Tianjin/00030/2020(H1N1)	99.67	99.86	A/swine/Liaoning/PJ43/2014(H1N1)	97.44	99.30		
HD21	A/swine/China/Qingdao/2018(H1N1)	97.49	99.02	A/swine/China/Qingdao/2018(H1N1)	97.49	99.02		
<b>HA</b>								
HD11	A/Tianjin/00030/2020(H1N1)	99.47	99.47	A/swine/Liaoning/CY102/2014(H1N1)	97.47	97.18		
HD21	A/Tianjin/00030/2020(H1N1)	98.71	98.59	A/swine/Liaoning/CY102/2014(H1N1)	97.30	97.35		
<b>NP</b>								
HD11	A/Tianjin/00030/2020(H1N1)	99.73	100.00	A/swine/Guangxi/NS1402/2012(H3N2)	97.80	98.20		
HD21	A/Tianjin/00030/2020(H1N1)	98.00	98.60	A/swine/Guangdong/NS2883/2012(H3N2)	97.80	99.00		
<b>NA</b>								
HD11	A/Shandong/00204/2021(H1N1)	99.57	99.36	A/swine/Ningjin/03/2014(H1N1)	97.02	95.96		
HD21	A/Sichuan/01208/2021(H1N1)	97.02	97.45	A/swine/Liaoning/PJ43/2014(H1N1)	96.67	95.74		
<b>M</b>								
HD11	A/Tianjin/00030/2020(H1N1)	99.69	99.70	A/swine/Shandong/LY142/2017(H1N1)	98.78	98.78		
	A/Sichuan/01208/2021(H1N1)							
HD21	A/Tianjin/00030/2020(H1N1)	98.47	98.48	A/swine/Shandong/LY142/2017(H1N1)	98.57	99.39		
	A/Sichuan/01208/2021(H1N1)	98.47	98.48					
<b>NS</b>								
HD11	A/Shandong/00204/2021(H1N1)	100.00	100.00	A/swine/Guangxi/1874/2012(H3N2)	97.97	96.43		
	A/Sichuan/01208/2021(H1N1)	100.00	100.00					
HD21	A/Hubei-Wujiagang/1324/2020(H1N1)	97.49	95.00	A/swine/China/Qingdao/2018(H1N1)	97.14	95.00		

\*HD11 is the isolate A/swine/Jiangsu/HD11/2020(H1N1); HD21 is the isolate A/swine/Anhui/HD21/2020(H1N1). GISAID, <https://www.gisaid.org>. HA, hemagglutinin; M, matrix; NA, neuraminidase; NP, nucleoprotein; NS, nonstructural protein; PA, polymerase acid; PB, polymerase basic.

A/Gansu-Xifeng/1143/2021(H1N1) and A/Gansu-Xifeng/1194/2021(H1N1) in PB1, PA, and NS gene trees. Taken together, HD11 and HD21 were both closest to contemporaneous human H1N1 strains, and they uniformly possessed the EA H1N1-like HA and NA genes, pandemic influenza-like RNP (PB2, PB1, PA, and NP) and M genes, and TR-like NS gene that made the G4 type gene constellation. We

observed that 2 additional swine reference viruses of A/swine/Shandong/LY142/2017(H1N1) and A/swine/China/Qingdao/2018(H1N1) assembled tightly with the HD11/HD21 cluster, further supporting the possibility of IAV interspecies transmission from swine to human.

The 2 G4 genotype EA H1N1 swine isolates both propagated well in specific-pathogen-free chicken

**Table 2.** Virus replication of 2 G4 Eurasian avian-like H1N1 swine isolates from pigs in China in vitro and in vivo\*

Virus strain	log <sub>10</sub> EID <sub>50</sub> /0.1 TCID <sub>50</sub> /0.1 mL		Virus growth in MDCK cells, mean titer ±SD, log <sub>10</sub> TCID <sub>50</sub> /0.1 mL†						Virus replication in infected mice, mean titer ±SD, log <sub>10</sub> copies/μL‡					
	0.1 mL	0.1 mL	12 hpi		24 hpi		36 hpi		3 dpi		5 dpi			
			12 hpi	24 hpi	36 hpi	48 hpi	60 hpi	Lung	Turb	Brain	Lung	Turb	Brain	
HD11	9.5	7.5	3.872§	5.041	7.000¶	5.556#	5.667**	5.679#	4.295**	2.495	3.828	2.385	2.703	
			±0.645	±0.219	±0.441	±0.096	±0.000	±0.355	±0.181	±0.318	±1.484	±0.219	±0.661	
HD21	9.375	5.769	3.055	4.389	4.556	4.556	4.444	3.894	2.008	1.667	4.550	2.334	2.692	
			±0.481	±0.096	±0.096	±0.096	±0.096	±0.195	±0.988	±0.537	±0.53	±0.221	±0.132	

\*We conducted 2-way analysis of variance in Prism software version 8 (GraphPad, <https://www.graphpad.com>) for virus titer comparison between HD11 and HD21 groups in each time point in cells or each tissue of the same sampling day in mice. dpi, days postinfection; EID<sub>50</sub>, 50% egg infectious dose; HD11, A/swine/Jiangsu/HD11/2020(H1N1); HD21, A/swine/Anhui/HD21/2020(H1N1); hpi, hours postinfection; TCID<sub>50</sub>, 50% tissue culture infectious dose (determined in MDCK cells); turb, turbinate.

†MDCK monolayers were infected with HD11 and HD21 at a multiplicity of infection (MOI) of 0.1. The virus titers of cell supernatants collected at different time points of 12, 24, 36, 48, and 60 h postinfection were determined via the TCID<sub>50</sub> assay in MDCK cells.

‡Three 6-week-old BALB/c mice per group challenged with 10<sup>6.0</sup> EID<sub>50</sub> virus in 50 μL volume were euthanized to collect tissue samples including the lung, turbinate, and brain for virus titration on 3 and 5 d postinoculation. The viral load expressed with virus copies in tissue homogenates was measured through the real-time quantitative reverse transcription PCR method as described (12).

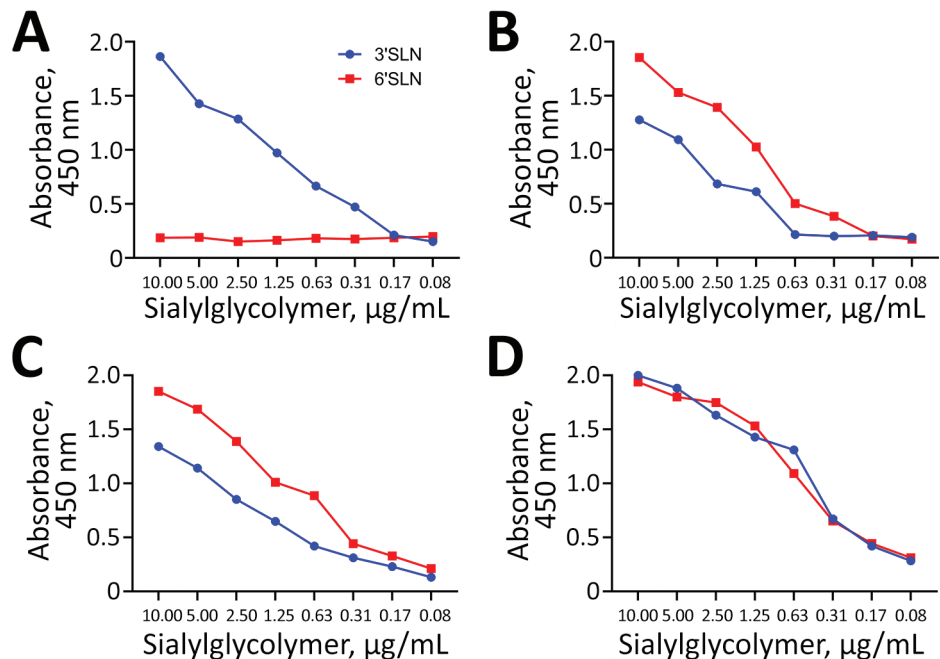
§p<0.05.

¶p<0.0001.

#p<0.01.

\*\*p<0.001.

**Figure 1.** Receptor-binding property of 2 G4 Eurasian avian-like influenza A(H1N1) swine isolates from pigs in China. A) The control virus A/mallard/Huadong/S/2005(H5N1) (HDS05) showed an absolute preference for avian-type SA $\alpha$ -2,3Gal. B) The control virus A/Jiangsu/202/2010(H3N2) (JS202) displayed double affinities to both human-type SA $\alpha$ -2,6Gal and avian-type SA $\alpha$ -2,3Gal, but with an overt bias toward SA $\alpha$ -2,6Gal. C) The tested virus A/swine/Jiangsu/HD11/2020(H1N1) (HD11) resembled the human-origin JS202 to possess an obviously advantageous avidity for SA $\alpha$ -2,6Gal over SA $\alpha$ -2,3Gal. D) The tested virus A/swine/Anhui/HD21/2020(H1N1) (HD21) exhibited comparable binding capacity to SA $\alpha$ -2,6Gal and SA $\alpha$ -2,3Gal without apparent preference. The solid-phase direct binding ELISA assay with the synthetic sialyl glycopolymers containing either 3'SLN-PAA and 6'SLN-PAA was applied to estimate the virus binding to avian-type SA $\alpha$ -2,3Gal and human-type SA $\alpha$ -2,6Gal, respectively. The data shown are representative of 3 independent binding experiments. SLN, sialyl-N-acetylglucosamine.



embryos with virus titers per 0.1mL  $>9 \log_{10}$  50% egg infectious dose (EID<sub>50</sub>) (Table 2). However, HD11 replicated much better than HD21 in MDCK cells through the titration of the 50% culture infectious dose (TCID<sub>50</sub>) value and virus growth at 12-hours intervals across 12–60 hours postinfection (hpi). At  $\geq 24$  hpi, HD11 had generated more than  $5 \log_{10}$  TCID<sub>50</sub> and reached a peak of  $7 \log_{10}$  TCID<sub>50</sub> at 36 hpi, where-

as the titer of HD21 virus remained at the relatively lower level  $<5 \log_{10}$  TCID<sub>50</sub> until the endpoint.

Subsequently, we conducted a solid-phase direct binding ELISA assay with the synthetic glycopolymer-based receptor mimics Neu5Aca2-3Galb1-4GlcNAcb(3-SLN)-PAA-biotin and Neu5Aca2-3Galb1-4GlcNAcb(6-SLN)-PAA-biotin (GlycoTech, <https://www.glycotech.com>) to evaluate

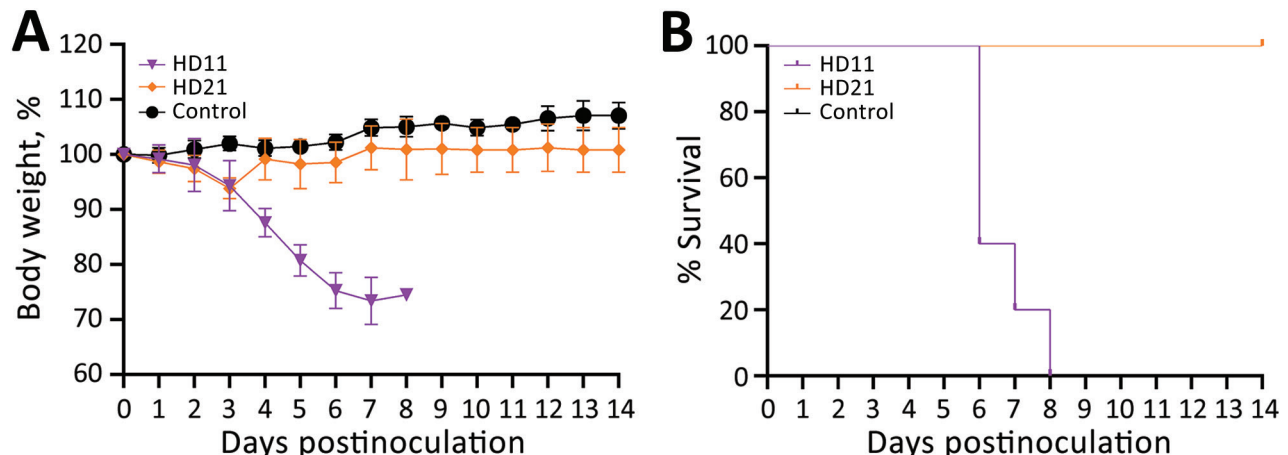


**Figure 2.** Pathogenicity of 2 G4 Eurasian avian-like influenza A(H1N1) swine isolates from pigs in China in BALB/c mice. A) Body weight change of infected mice. B) Survival curve of infected mice. Two groups of five 6-week-old BALB/c mice were inoculated intranasally with A/swine/Jiangsu/HD11/2020(H1N1) (HD11) or A/swine/Anhui/HD21/2020(H1N1) (HD21) at a dose of  $10^6$  50% egg infectious dose/50  $\mu$ L. Another 5 mice mock-infected with phosphate-buffered saline were served as control. Body weight change and survival rate were recorded daily until 14 days postinoculation, and mice that lost  $\geq 25\%$  of the initial body weight were humanely euthanized.

the viral receptor-binding preference as previously described (13). We used 1 avian H5N1 virus and 1 human seasonal H3N2 virus as controls; the avian virus displayed a complete 3-sialyl-N-acetylglucosamine (SLN) affinity, whereas the human virus possessed a dual binding property to both 3-SLN and the more advantageous 6-SLN (Figure 1). Unlike HD21, which was endowed with comparable avidity between 3-SLN and 6-SLN, HD11 resembled the binding feature of the human-origin H3N2 virus that preferentially binds the human-type SA $\alpha$ -2,6Gal (Figure 1).

We then investigated the pathogenicity of HD11 and HD21 in mice. We infected 6-week-old BALB/c mice in groups of 5 intranasally with  $10^{6.0}$  EID<sub>50</sub> virus dose or mock-inoculated them with phosphate-buffered saline (PBS). We monitored body weight changes and clinical symptoms of the mice daily for 14 days. We humanely euthanized an additional 3 challenged mice per group and analyzed them for virus load in tissues at 3 and 5 days postinfection (dpi). Mice in the control group displayed a steady increase in body weight, the HD21 group experienced a slightly transient weight loss on 3 dpi, and all mice survived during the entire experiment (Figure 2). In contrast, HD11 resulted in a steady decrease in body weights starting at 1 dpi, and all died within 8 days. In addition, we observed that both HD11 and HD21 replicated efficiently in the lungs without prior adaptation and readily disseminated into nasal turbinates and the brain (Table 2). Of note, the virus load in respiratory tissues of HD11-infected mice was significantly higher ( $p < 0.01$  in lungs and  $p < 0.001$  in turbinates) than that of HD21-infected mice on 3 dpi. On 5 dpi, we observed no significant difference in virus titers in the 3 tissues of the mice infected with these 2 isolates. Moreover, HD11 infections increased the mRNA levels of inflammatory cytokines, including interleukin 6 and 10, interferon  $\beta$  and  $\gamma$ , MX1, and C-X-C motif chemokine ligand 10 11 on 3 dpi, 5 dpi, or both, more dramatically than HD21 virus. Both HD21 and HD11 infections increased tumor necrosis factor  $\alpha$  expression at relatively low levels (Appendix Figure 2).

## Conclusions

Homology alignment and phylogenetic tree construction analysis suggest that HD11 and HD21, two G4 EA H1N1 swine IAVs isolated in 2020 in China, are strongly related to recent human-origin EA H1N1 viruses. In particular, HD11 had higher affinity for human-type 6-SLN at the level that is equivalent to the human seasonal H3N2 virus. Moreover, HD11 replicated much faster in vitro in MDCK cells and in vivo

in the lung than di HD21 and was highly pathogenic to BALB/c mice, as evidenced by its lethality, higher viral loads in pulmonary tissues, and higher levels of inflammatory cytokines in the lung. We propose that the HD11-like G4 swine isolates whose genomic sequences share great homology with that of contemporary human EA H1N1 viruses may lead to interspecies transmission. Therefore, the public health threat from the zoonotic G4 EA H1N1 viruses should not be underestimated.

## Acknowledgments

We thank Xiulong Xu for revising and editing the manuscript.

This work was supported by the National Key Research and Development Program of China (no. 2021YFD1800202), the National Natural Science Foundation of China (no. 32072892), the Jiangsu Provincial Postdoctoral Science Foundation (no. 1501075C), the Priority Academic Program Development of Jiangsu Higher Education Institutions, the Jiangsu Qinglan Project, and the High-end talent support program of Yangzhou University.

## About the Author

Dr. Gu is a faculty member at College of Veterinary Medicine, Yangzhou University. Her research primarily focuses on the epidemiology of zoonotic influenza viruses and the mechanisms of virus evolution.

## References

1. Crisci E, Mussá T, Fraile L, Montoya M. Review: influenza virus in pigs. *Mol Immunol*. 2013;55:200–11. <https://doi.org/10.1016/j.molimm.2013.02.008>
2. Nelson MI, Vincent AL. Reverse zoonosis of influenza to swine: new perspectives on the human-animal interface. *Trends Microbiol*. 2015;23:142–53. <https://doi.org/10.1016/j.tim.2014.12.002>
3. Chastagner A, Enouf V, Peroz D, Hervé S, Lucas P, Quéguiner S, et al. Bidirectional human–swine transmission of seasonal influenza A(H1N1)pdm09 virus in pig herd, France, 2018. *Emerg Infect Dis*. 2019;25:1940–3. <https://doi.org/10.3201/eid2510.190068>
4. Deng YM, Wong FYK, Spirason N, Kaye M, Beazley R, Grau MLL, et al. Locally acquired human infection with swine-origin influenza A(H3N2) variant virus, Australia, 2018. *Emerg Infect Dis*. 2020;26:143–7. <https://doi.org/10.3201/eid2601.191144>
5. Anderson TK, Chang J, Arendsee ZW, Venkatesh D, Souza CK, Kimble JB, et al. Swine influenza A viruses and the tangled relationship with humans. *Cold Spring Harb Perspect Med*. 2021;11:a038737. <https://doi.org/10.1101/cshperspect.a038737>
6. Feng Z, Zhu W, Yang L, Liu J, Zhou L, Wang D, et al. Epidemiology and genotypic diversity of Eurasian avian-like H1N1 swine influenza viruses in China. *Virol Sin*. 2021;36:43–51. <https://doi.org/10.1007/s12250-020-00257-8>
7. Li X, Guo L, Liu C, Cheng Y, Kong M, Yang L, et al. Human infection with a novel reassortant Eurasian-avian lineage

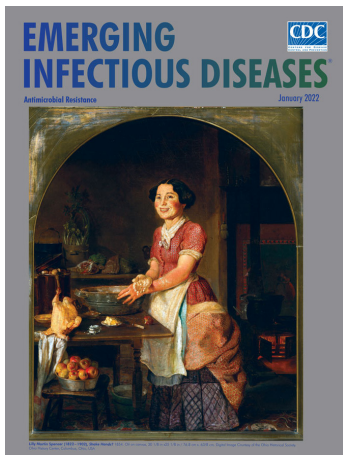
- swine H1N1 virus in northern China. *Emerg Microbes Infect.* 2019;8:1535–45. <https://doi.org/10.1080/22221751.2019.1679611>
8. Li Z, Zhao X, Huang W, Yang L, Cheng Y, Tan M, et al. Etiological characteristics of the first human infection with the G4 genotype Eurasian avian-like H1N1 swine influenza virus in Yunnan province, China [in Chinese]. *Chinese Journal of Virology.* 2022;38:290–7.
  9. World Health Organization. Influenza at the human-animal interface summary and assessment, 1 October 2021. 2021 [cited 2021 Dec 14]. <https://www.who.int/publications/m/item/influenza-at-the-human-animal-interface-summary-and-assessment-1-october-2021>
  10. Yang H, Chen Y, Qiao C, He X, Zhou H, Sun Y, et al. Prevalence, genetics, and transmissibility in ferrets of Eurasian avian-like H1N1 swine influenza viruses. *Proc Natl Acad Sci U S A.* 2016;113:392–7. <https://doi.org/10.1073/pnas.1522643113>
  11. Sun H, Xiao Y, Liu J, Wang D, Li F, Wang C, et al. Prevalent Eurasian avian-like H1N1 swine influenza virus with 2009 pandemic viral genes facilitating human infection. *Proc Natl Acad Sci U S A.* 2020;117:17204–10. <https://doi.org/10.1073/pnas.1921186117>
  12. Chen K, Kong M, Liu J, Jiao J, Zeng Z, Shi L, et al. Rapid differential detection of subtype H1 and H3 swine influenza viruses using a TaqMan-MGB-based duplex one-step real-time RT-PCR assay. *Arch Virol.* 2021;166:2217–24. <https://doi.org/10.1007/s00705-021-05127-6>
  13. Yamada S, Suzuki Y, Suzuki T, Le MQ, Nidom CA, Sakai-Tagawa Y, et al. Haemagglutinin mutations responsible for the binding of H5N1 influenza A viruses to human-type receptors. *Nature.* 2006;444:378–82. <https://doi.org/10.1038/nature05264>

Address for correspondence: Xiufan Liu, Animal Infectious Diseases Laboratory, College of Veterinary Medicine, Yangzhou University, 48 East Wenhui Road, Yangzhou, Jiangsu 225009, China; email: xfliu@yzu.edu.cn

January 2022

## Antimicrobial Resistance

- Outbreak of Mucormycosis in Coronavirus Disease Patients, Pune, India
- Severe Acute Respiratory Syndrome Coronavirus 2 and Respiratory Virus Sentinel Surveillance, California, USA, May 10, 2020–June 12, 2021
- Using the Acute Flaccid Paralysis Surveillance System to Identify Cases of Acute Flaccid Myelitis, Australia, 2000–2018
- Fungal Infections Caused by *Kazachstania* spp., Strasbourg, France, 2007–2020
- Multistate Outbreak of SARS-CoV-2 Infections, Including Vaccine Breakthrough Infections, Associated with Large Public Gatherings, United States
- Potential Association of Legionnaires' Disease with Hot Spring Water, Hot Springs National Park and Hot Springs, Arkansas, USA, 2018–2019
- Mask Effectiveness for Preventing Secondary Cases of COVID-19, Johnson County, Iowa, USA



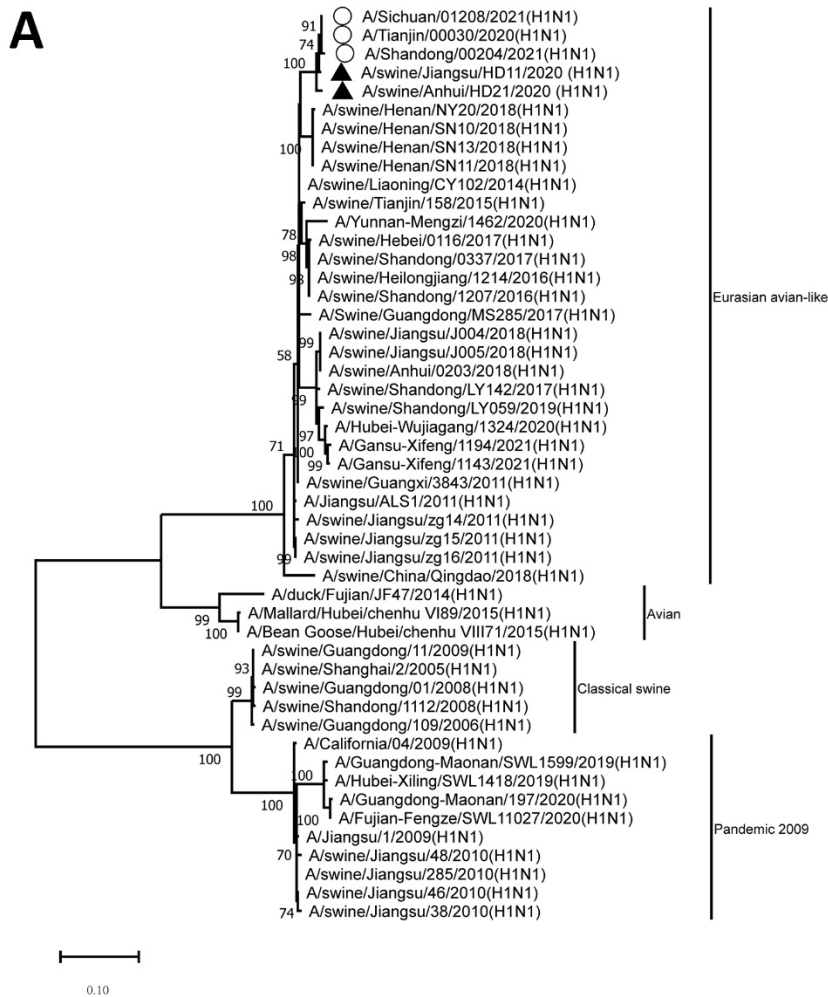
- Transmission Dynamics of Large Coronavirus Disease Outbreak in Homeless Shelter, Chicago, Illinois, USA, 2020
- Risk Factors for SARS-CoV-2 Infection Among US Healthcare Personnel, May–December 2020
- Systematic Genomic and Clinical Analysis of Severe Acute Respiratory Syndrome Coronavirus 2 Reinfections and Recurrences Involving the Same Strain
- High-Level Quinolone-Resistant *Haemophilus haemolyticus* in Pediatric Patient with No History of Quinolone Exposure
- New Sequence Types and Antimicrobial Drug-Resistant Strains of *Streptococcus suis* in Diseased Pigs, Italy, 2017–2019
- Invasive Multidrug-Resistant *emm93.0 Streptococcus pyogenes* Strain Harboring a Novel Genomic Island, Israel, 2017–2019
- Coronavirus Disease Spread during Summer Vacation, Israel, 2020
- Extensively Drug-Resistant Carbapenemase-Producing *Pseudomonas aeruginosa* and Medical Tourism from the United States to Mexico, 2018–2019
- Effects of Nonpharmaceutical COVID-19 Interventions on Pediatric Hospitalizations for Other Respiratory Virus Infections, Hong Kong
- Global Genome Diversity and Recombination in *Mycoplasma pneumoniae*

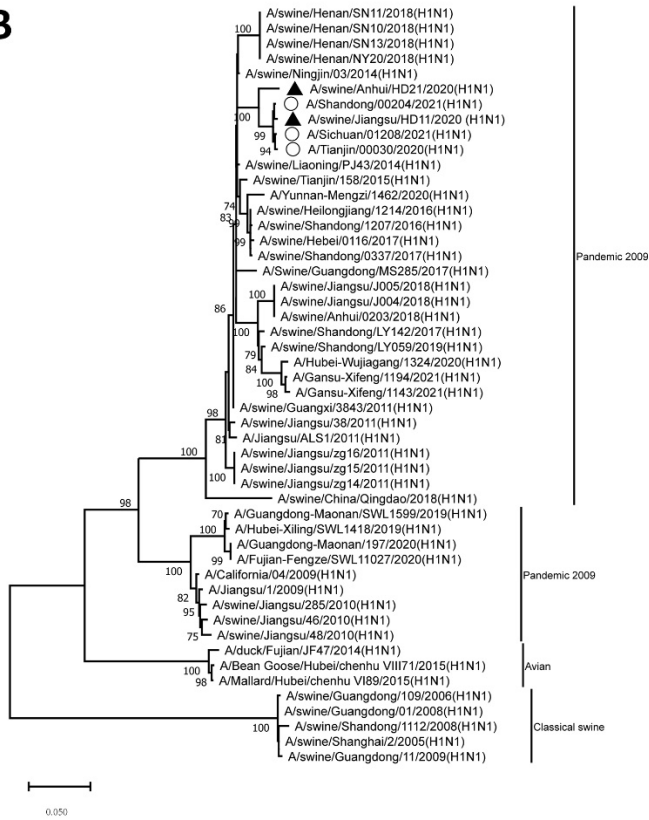
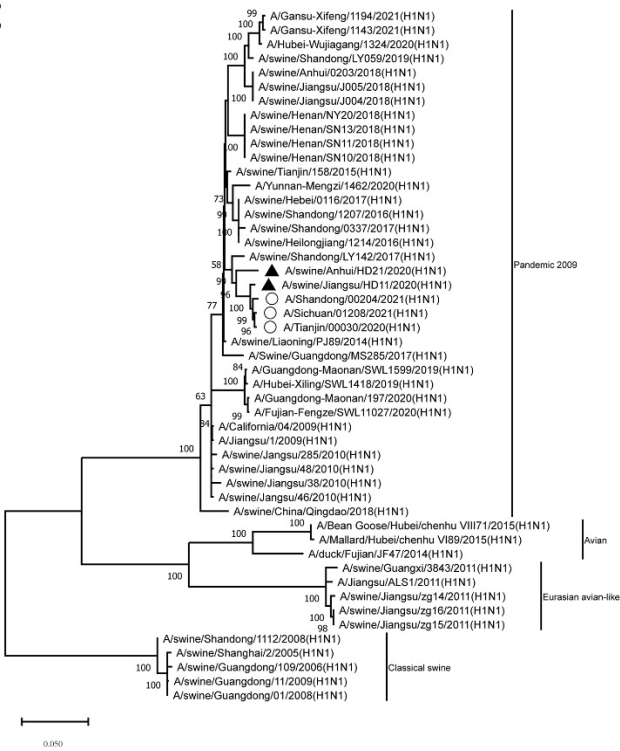
**EMERGING  
INFECTIOUS DISEASES**

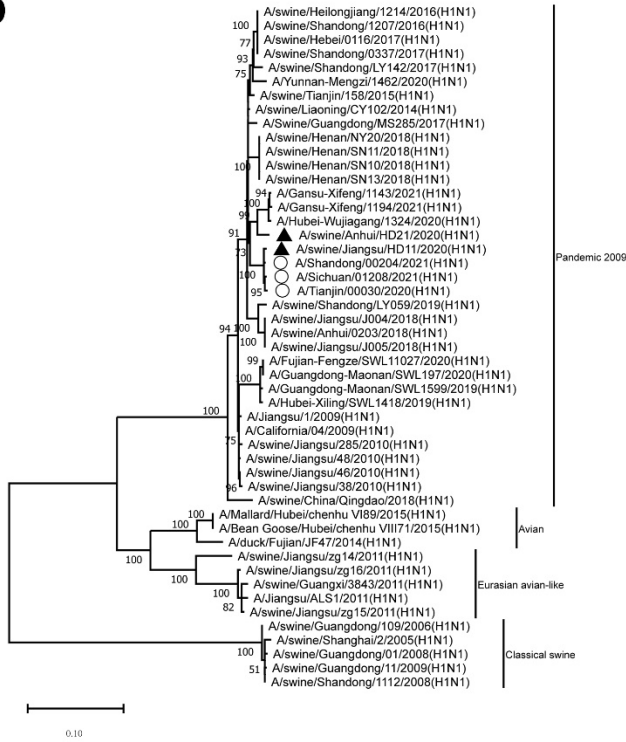
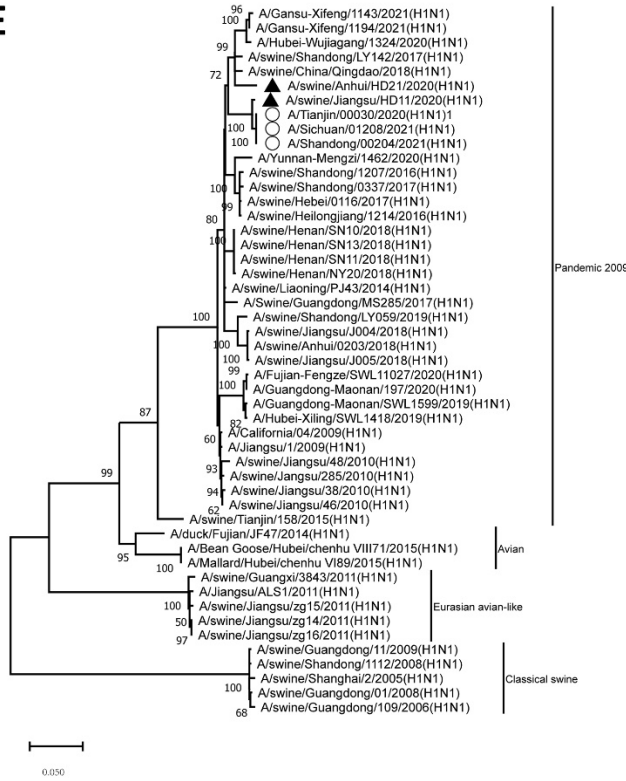
To revisit the January 2022 issue, go to:  
<https://wwwnc.cdc.gov/eid/articles/issue/28/1/table-of-contents>

# Zoonotic Threat of G4 Genotype Eurasian Avian-Like Swine Influenza A(H1N1) Viruses, China, 2020

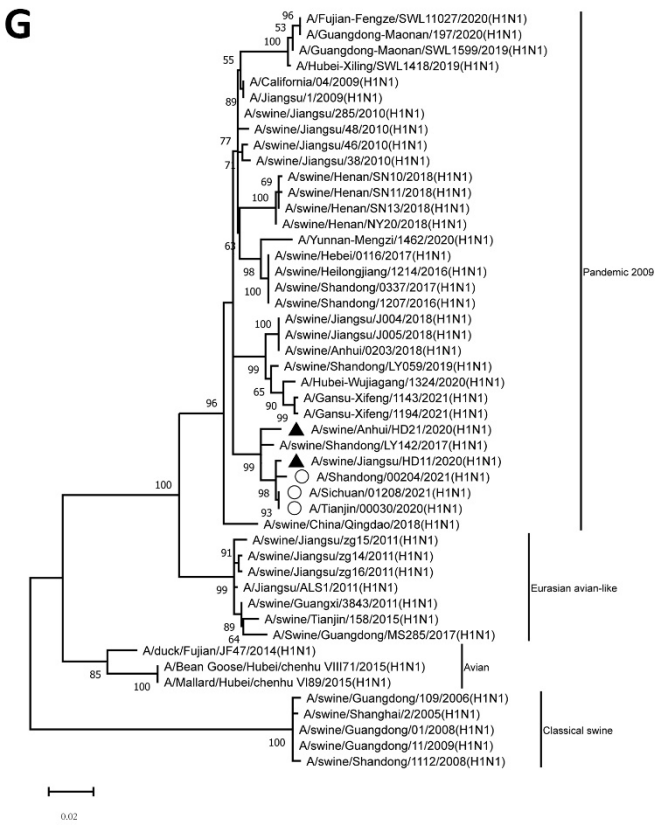
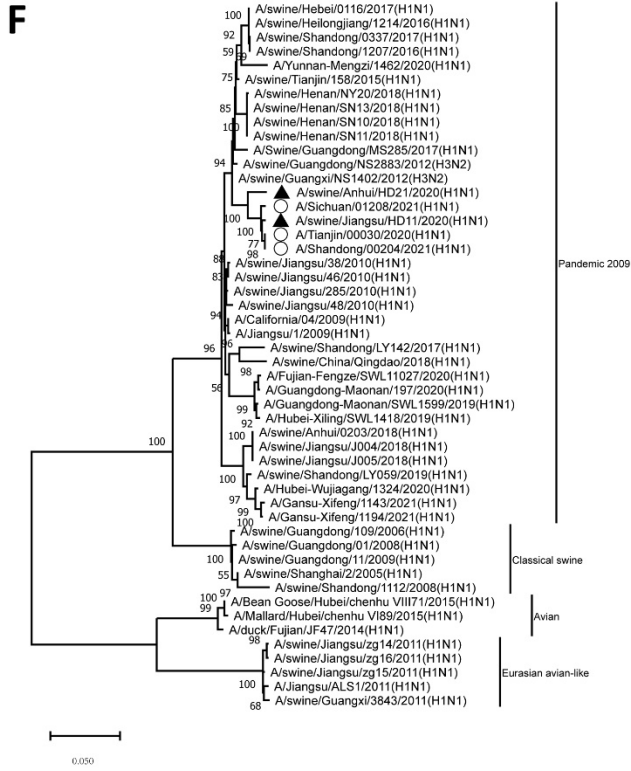
## Appendix

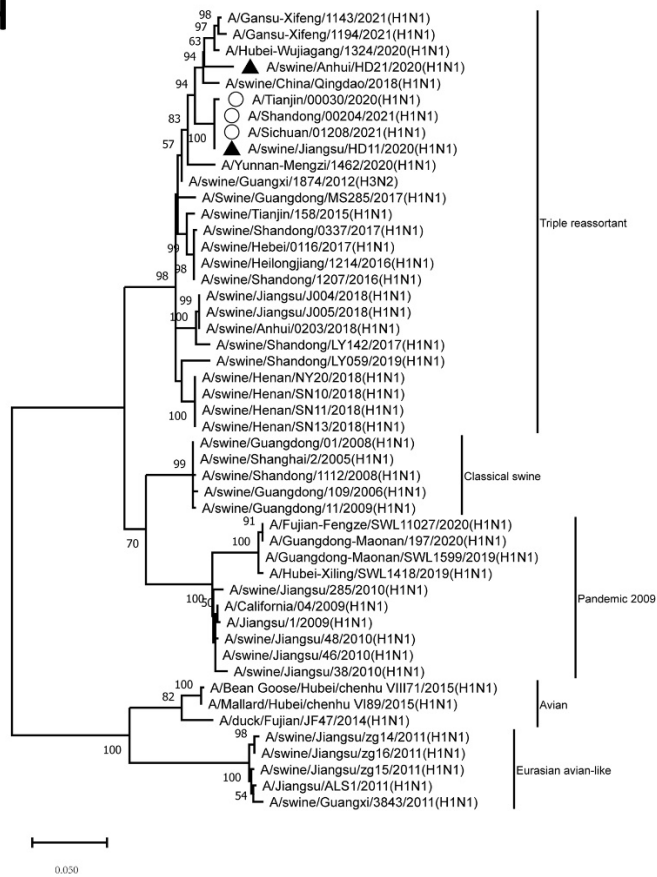


**B****C**

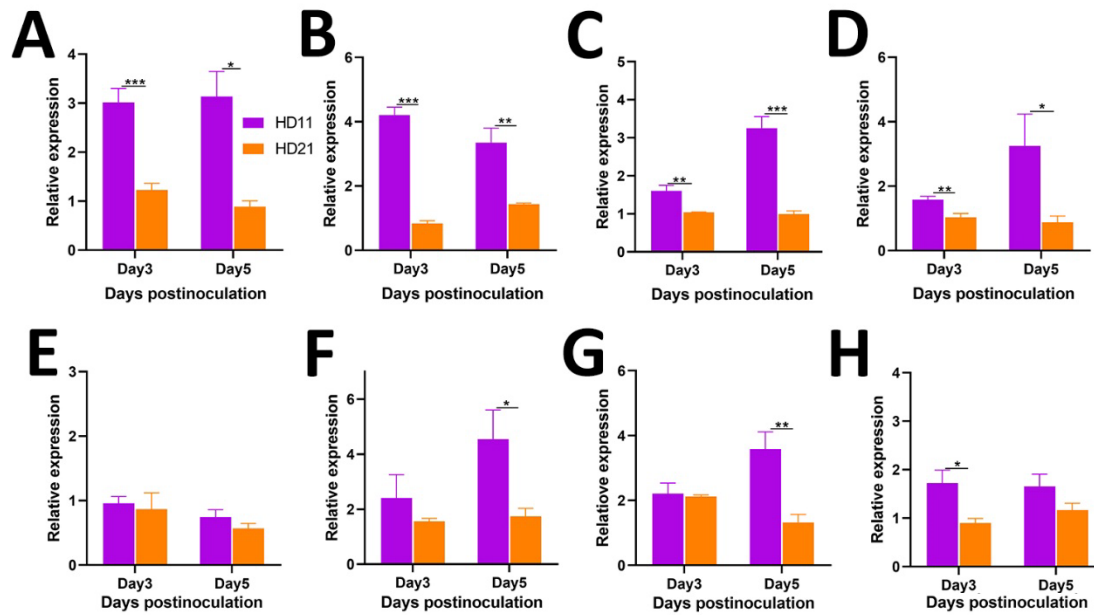
**D****E**





**H**

Black triangles indicate G4 EA H1N1 swine isolates of *A/swine/Jiangsu/HD11/2020(H1N1)* [HD11] and *A/swine/Anhui/HD21/2020(H1N1)* [HD21] in this study. Reference sequences of Eurasian avian-like, Pandemic 2009, Classical swine, Triple reassortant and avian H1N1 subtype IAV lineages were retrieved from the GISAID platform (<http://www.gisaid.org>), especially those human viruses showing consistent homology with HD11 and HD21 in all 8 genes; hollow circles indicate those strains. Each maximum-likelihood tree was generated using the MEGA software version 11 (<http://www.megasoftware.net>). We evaluated tree topology by bootstrap resampling method with 1,000 replicates. Scale bar indicates nucleotide substitutions per site.



**Appendix Figure 2.** The expression level of inflammatory cytokines induced by 2 G4 Eurasian avian-like H1N1 swine isolates in mouse lungs. Groups of six 6-week-old BABL/c mice were intranasally inoculated with  $10^{6.0}$  EID<sub>50</sub> A/swine/Jiangsu/HD11/2020(H1N1) [HD11] or A/swine/Anhui/HD21/2020(H1N1) [HD21]. On 3 and 5 days postinoculation, 3 mice from each group were euthanized to collect the lungs for homogenate preparation. We evaluated relative mRNA expression levels of IL-6 (A), IL-10 (B), IFN-β (C), INF-γ (D), TNF-α (E), MX1 (F), CXCL-10 (G), and CXCL-11 (H) in the infected mouse lungs by the real-time quantitative RT-PCR method. All values were normalized to GAPDH and expressed as fold change against controls. Values were shown as mean±SD from 3 independent determinations. (\*, p<0.05; \*\*, p<0.01; \*\*\*, p<0.001).